arXiv:1606.07171v1 [hep-ph] 23 Jun 2016

CTPU-16-18
IPMU16-0084

Confronting diphoton resonance with cascade decays in warped gravity

Barry M. Dillon[1,*], **Chengcheng Han**[2,$], **Hyun Min Lee**[3,†], **and Myeonghun Park**[4,‡]

[1] *Department of Physics and Astronomy, University of Sussex, Brighton BN1 9QH, UK.*
[2] *Kavli Institute for the Physics and Mathematics of the Universe (WPI), The University of Tokyo, Japan.*
[3] *Department of Physics, Chung-Ang University, Seoul 06974, Korea.*
[4] *Center for Theoretical Physics and Universe, Institute for Basic Science (IBS), Daejeon 34051, Korea.*

Abstract

We consider a Kaluza-Klein (KK) graviton interpretation of the diphoton excesses observed recently at the LHC. The radion, the modulus of extra dimension, appears naturally light due to classical scale invariance in this scenario. Thus, due to the presence of a sizable wavefunction overlap in the extra dimension between the KK graviton and the radion, the KK graviton can decay largely into a pair of radions, each of which decays into a pair of collimated photons, the so called photon-jet. We discuss the photon-jet scenario in setups with warped extra dimension that are consistent with current limits from direct searches and electroweak precision data. One scenario is with suppressed couplings of the KK graviton to the Higgs and fermions, and another scenario is a holographic composite Higgs model with large couplings of the KK graviton to Higgs and top quark included. We discuss the bounds on the light radion and the possibility of distinguishing the photon-jet scenario with the angular distributions of photons in the LHC Run 2.

[*]Email: b.dillon@sussex.ac.uk
[$]Email: chengcheng.han@ipmu.jp
[†]Email: hminlee@cau.ac.kr
[‡]Email: parc.ctpu@gmail.com

1 Introduction

Excesses at 750 GeV in the diphoton invariant mass spectrum observed at the LHC have recently drawn huge attention from particle physics community. Significances for the excesses are 3.9σ and 3.4σ in ATLAS and CMS collaborations [1], respectively, depending on the assumption of the resonance width, but they have not reached the level of discovery yet. Nonetheless, there is a growing interest in the development of the diphoton excesses from the upcoming LHC Run 2 that have started operating from early May.

In most of theory interpretations of the diphoton excesses in physics Beyond the Standard Model (BSM), one relies upon the presence of scalar or tensor resonances with 750 GeV mass [2,4,5] that are produced from gluon fusion[1] and decay into a pair of photons. Therefore, either a large gluon or photon coupling is necessary, depending on whether we take a large production cross section via gluons or a large decay branching fraction of the resonance to photons. But, the former case with a large gluon coupling is constrained by dijet searches as well as searches for other decay modes of the resonance such as $WW, ZZ, Z\gamma$ and dilepton, etc [2]. As a result, the case with a sizable photon coupling is favored by the LHC data.

There is another option for explaining the diphoton excesses in terms of collimated photons or photon-jets [6–8], that come from the decay of intermediate light states that the 750 GeV resonance decays into. Since the efficiency that one or both of collimated photons are converted into a pair of electron and positron at the LHC can be sizable [8], the photon-jet scenario is soon expected to be distinguished from the case with single photons.

In this work, we consider a Kaluza-Klein(KK) graviton with 750 GeV mass [4, 5] and a light radion in the Randall-Sundrum(RS) model [10]. However we consider general couplings on the branes and their effects on the phenomenology of the graviton and radion. As both the KK graviton and the radion are localized towards the IR brane [11–13], there is a sizable overlap between their wavefunctions in the extra dimension, so the KK graviton can decay largely into a pair of radions. We assume that the rest of the SM fields, in particular, light fermions, are localized towards the UV brane, in order to avoid strong bounds from dijet and/or dilepton bounds. In principle, the KK graviton could have sizeable couplings to heavy quarks and the Higgs fields. For simplicity, we focus on the case where the KK graviton couples more to the transverse polarizations of gauge bosons than to the rest of the SM fields, but we also mention the case with sizable couplings of the KK graviton to heavy quarks and the SM Higgs fields in the context of the Composite Higgs scenario. We first discuss the effects of the couplings between KK graviton and radion for the diphoton interpretation in a model independent way and then illustrate specific models such the minimal RS model and its extensions.

In order for photon-jets to contribute to the diphoton excesses dominantly, we need a large decay branching fraction of the light radion into a photon pair and the radion must decay within the ECAL. In the case that the Yukawa couplings of the radion to light fermions are suppressed due to their localization, a light radion with mass smaller than twice the pion mass can decay mostly into a photon pair. We also discuss the effect of a large brane kinetic term for the hypercharge gauge boson on the couplings to radion and the KK graviton as

[1] We note that the $b\bar{b}$ production channel can also give a dominant contribution to the production cross section for heavy Higgs bosons [3], being compatible with the $b\bar{b}$ bound from the LHC Run 1.

well as the first KK mass of hypercharge gauge boson, as compared to those of gluons with no or small brane kinetic terms. In this regard, we explore the phenomenologically viable parameter space of radion couplings for the photon-jet interpretation of the excess.

The paper is organized as follows. We begin with a general discussion on the diphoton interpretation in the system with a KK graviton and radion and discuss the bounds on a light radion. Next we consider specific examples in the RS model and its extensions and discuss the phenomenology of photon-jets. Then we take the radion as a mediator of dark matter and discuss the invisible decay of the KK graviton. Finally, conclusions are drawn.

2 Diphoton bump from spin-0 and spin-2 particles

We assume that the diphoton resonance observed at the LHC is solely of geometrical origin from the extra dimension or its dual conformal field theories. In this case, the radion, the volume modulus of the extra dimension and/or the KK graviton are good candidates for the diphoton resonance. The couplings of the radion and the KK graviton to the SM particles are determined by the wave-function overlaps in the extra dimension. Although the wave functions of the radion and the KK graviton are fixed for a given background geometry, the counterparts of the SM particles are model-dependent.

2.1 Effective interactions for spin-0 and spin-2 fields

We consider the effective interactions of a radion-like spin-0 field, r, and a graviton-like spin-2 field, $G_{\mu\nu}$, to SM fields, and their self-interactions, as follows,

$$\begin{aligned}
\mathcal{L}_{\text{eff}} \;=\; & \frac{c_1}{\Lambda}G^{\mu\nu}\Big(\frac{1}{4}\eta_{\mu\nu}B_{\lambda\rho}B^{\lambda\rho}+B_{\mu\lambda}B^{\lambda}{}_{\nu}\Big)+\frac{c_2}{\Lambda}G^{\mu\nu}\Big(\frac{1}{4}\eta_{\mu\nu}W_{\lambda\rho}W^{\lambda\rho}+W_{\mu\lambda}W^{\lambda}{}_{\nu}\Big)\\
&+\frac{c_3}{\Lambda}G^{\mu\nu}\Big(\frac{1}{4}\eta_{\mu\nu}g_{\lambda\rho}g^{\lambda\rho}+g_{\mu\lambda}g^{\lambda}{}_{\nu}\Big)\\
&-\frac{ic_f}{2\Lambda}G^{\mu\nu}\left(\bar{f}\gamma_\mu\overleftrightarrow{D}_\nu f-\eta_{\mu\nu}\bar{f}\gamma_\rho\overleftrightarrow{D}^\rho f\right)\\
&+\frac{c_H}{\Lambda}G^{\mu\nu}\left(2(D_\mu H)^\dagger D_\nu H-\eta_{\mu\nu}\left((D_\rho H)^\dagger D^\rho H-V(H)\right)\right)\\
&-\frac{r}{\Lambda}\left(d_1B_{\lambda\rho}B^{\lambda\rho}+d_2W_{\lambda\rho}W^{\lambda\rho}+d_3g_{\lambda\rho}g^{\lambda\rho}\right)\\
&+\frac{d_f}{\Lambda}\,m_f r\bar{f}f+\frac{4d_H}{\Lambda}\,m_H^2 r|H|^2-\frac{d_V}{\Lambda}\,r(m_Z^2Z_\mu Z^\mu+2m_W^2W_\mu W^\mu)\\
&-\frac{c_{rr}}{\Lambda}\left[G^{\mu\nu}\partial_\mu r\partial_\nu r+\frac{3}{2}G(\partial r)^2+r^2(\partial_\mu\partial_\nu G^{\mu\nu}-\Box G)\right] \qquad (1)
\end{aligned}$$

where $B_{\mu\nu}, W_{\mu\nu}, G_{\mu\nu}$ are the field strength tensors for $U(1)_Y, SU(2)_L, SU(3)_C$ gauge fields, respectively, f is the SM fermion, H is the Higgs doublet. Here, we note that $c_i (i=1,2,3)$, c_f, and c_H are constant dimensionless couplings for the KK graviton while $d_i (i=1,2,3)$, d_f, d_H, d_V, and c_{rr} are those for the radion. The couplings between the KK graviton and the radion are derived from the 5D Einstein-Hilbert action and the detailed derivation of those gravity self-interactions in the 5D warped geometry can be found in the appendix.

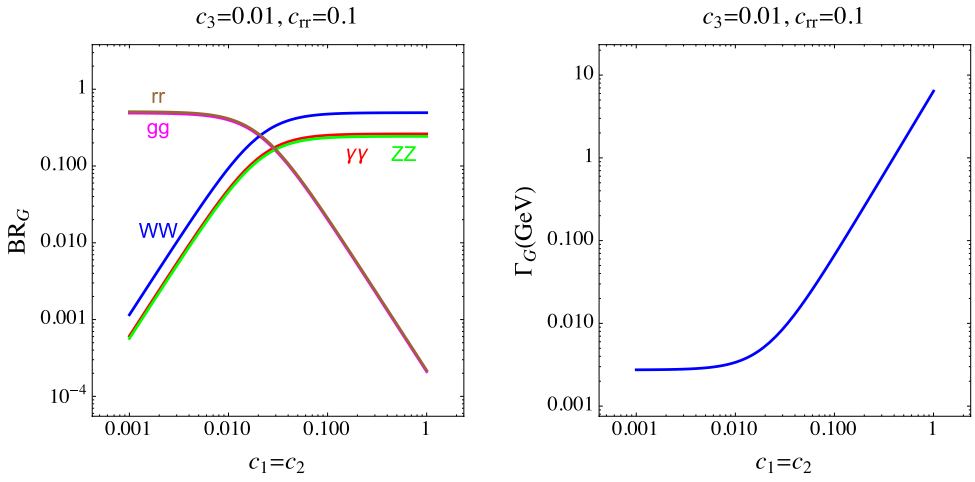

Figure 1: Decay branching fractions and total decay width of KK graviton as a function of $c_1 = c_2$. We have taken $\Lambda = 1\,\text{TeV}$, $c_3 = 0.01$ and $c_{rr} = 0.1$, and $c_H = c_f = 0$.

Then, the partial decay rates of the KK graviton [14] are given by

$$
\begin{aligned}
\Gamma_G(gg) &= \frac{c_{gg}^2 m_G^3}{10\pi\Lambda^2}, \qquad \Gamma_G(\gamma\gamma) = \frac{c_{\gamma\gamma}^2 m_X^3}{80\pi\Lambda^2}, \\
\Gamma_G(ZZ) &= \frac{m_G^3}{80\pi\Lambda^2}\sqrt{1-4r_Z}\left(c_{ZZ}^2 + \frac{c_H^2}{12} + \frac{r_Z}{3}\left(3c_H^2 - 20c_H c_{ZZ} - 9c_{ZZ}^2\right)\right. \\
&+ \left.\frac{2r_Z^2}{3}\left(7c_H^2 + 10c_H c_{ZZ} + 9c_{ZZ}^2\right)\right), \\
\Gamma_G(WW) &= \frac{m_G^3}{40\pi\Lambda^2}\sqrt{1-4r_W}\left(c_{WW}^2 + \frac{c_H^2}{12} + \frac{r_W}{3}\left(3c_H^2 - 20c_H c_{WW} - 9c_{WW}^2\right)\right. \\
&+ \left.\frac{2r_W^2}{3}\left(7c_H^2 + 10c_H c_{WW} + 9c_{WW}^2\right)\right), \\
\Gamma_G(Z\gamma) &= \frac{c_{Z\gamma}^2 m_G^3}{40\pi\Lambda^2}(1-r_Z)^3\left(1 + \frac{r_Z}{2} + \frac{r_Z^2}{6}\right),
\end{aligned}
$$

$$
\begin{aligned}
\Gamma_G(f\bar{f}) &= \frac{N_c c_f^2 m_G^3}{320\pi\Lambda^2}(1-4r_f)^{3/2}(1+8r_f/3), \\
\Gamma_G(hh) &= \frac{c_H^2 m_G^3}{960\pi\Lambda^2}(1-4r_h)^{5/2}, \\
\Gamma_G(rr) &= \frac{c_{rr}^2 m_G^3}{960\pi\Lambda^2}(1-4r_r)^{5/2}
\end{aligned}
\tag{2}
$$

where $c_{\gamma\gamma} = s_\theta^2 c_2 + c_\theta^2 c_1$, $c_{ZZ} = c_\theta^2 c_2 + s_\theta^2 c_1$, $c_{Z\gamma} = s_\theta c_\theta (c_2 - c_1)$, $c_{gg} = c_3$, $c_{WW} = 2c_2$, $r_i = (m_i/m_G)^2$, and $m_G = 750$ GeV is the lightest KK graviton mass.

In Fig. 1, we depict the decay branching fractions and total decay rate of the KK graviton by assuming that the Higgs fields and the SM fermions have suppressed couplings to the KK graviton, namely, $c_H = c_f = 0$. Then, choosing $c_1 = c_2$, the KK graviton decays into

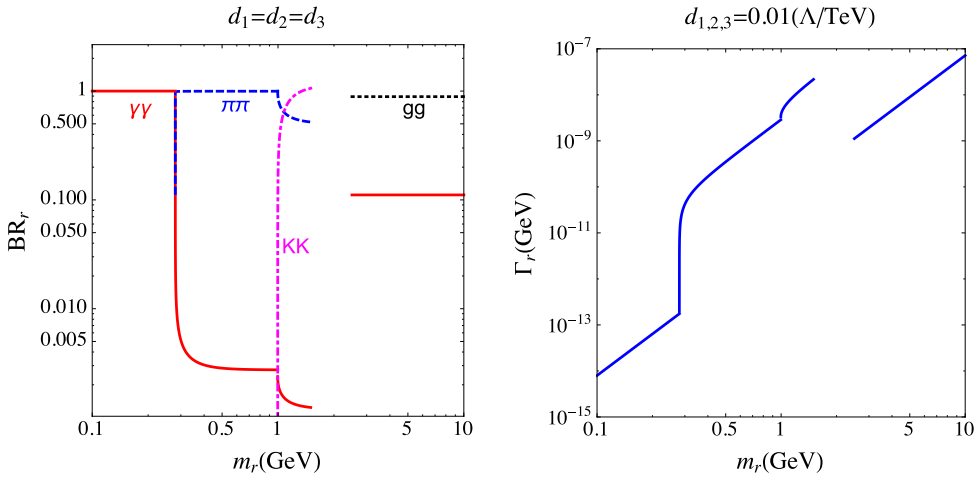

Figure 2: Decay branching fractions and total decay width of radion as a function of radion mass. We have taken $d_1 = d_2 = d_3 = 0.01(\Lambda/\text{TeV})$.

$WW, ZZ, \gamma\gamma, gg$ or rr. We took $c_3 = 0.01$ and $c_{rr} = 0.1$ and assumed that there is no invisible decay of the KK graviton. In a later section, we will also show the effects of the invisible decay into a pair of dark matter particles.

When the radion couplings to light fermions are suppressed, with a light radion [2], the only relevant decay rates for the radion are to a pair of photons or gluons,

$$\Gamma_r(\gamma\gamma) = \frac{d_{\gamma\gamma}^2 m_r^3}{4\pi\Lambda^2}, \tag{3}$$

$$\Gamma_r(gg) = \frac{2d_{gg}^2 m_r^3}{\pi\Lambda^2} \tag{4}$$

where $d_{\gamma\gamma} = d_1 \cos^2\theta_W + d_2 \sin^2\theta_W$ and $d_{gg} = d_3$. When the radion is lighter than $2m_\pi < m_r \lesssim 1.5\,\text{GeV}$, we also need to include the radion decays into a pair of mesons in chiral perturbation theory, instead of the decay into a gluon pair. For instance, the decay rate of the radion into a pair of pions ($\pi^a\pi^a$ with $a = 1, 2, 3$) is

$$\Gamma_r(\pi^a\pi^a) = \frac{4\pi}{b^2\alpha_S^2(M_Z)} \frac{d_{gg}^2(M_Z) m_r^3}{\Lambda^2} \left(1 + \frac{m_\pi^2}{m_r^2}\right)^2 \sqrt{1 - \frac{4m_\pi^2}{m_r^2}} \tag{5}$$

with the coefficient of the QCD beta function being $b = \frac{29}{3}(9)$ for $u, d, (s)$ light quarks in chiral perturbation theory. Here, the radion effective gluon coupling, $d_{gg}(M_Z)$, and the strong gauge coupling, $\alpha_S(M_Z) = 0.118$, can be chosen at Z pole, near the matching scale to the extra dimension. We note that the loop contributions of heavy quarks to the radion couplings are taken to be absorbed into the bulk radion coupling, which is taken to be dominant in the following discussion. In Fig. 2, we show the decay branching fractions and total decay rate of the radion by assuming that the Higgs fields and the SM fermions have suppressed couplings to the KK graviton, namely, $d_H = d_V = d_f = 0$. Here, we have chosen $d_1 = d_2 = d_3 =$

[2] The possibility of having a heavy radion with 750 GeV mass for diphoton excesses was also considered [15].

$0.01(\Lambda/\text{TeV})$ for $\Lambda = 1\,\text{TeV}$. We note that the branching fractions or the total decay rate of the radion are not shown for $1.5\,\text{GeV} < m_r < 2.5\,\text{GeV}$, for which either descriptions in terms of mesons or quarks/gluons are not quite correct.

In the following discussion we consider the case where the spin-2 resonance couples more strongly to transverse polarizations of gauge bosons than to the rest of the SM fields and focus on photon and gluon couplings to the spin-2 resonance after electroweak symmetry breaking. In the warped model, we assume that the majority of the SM fields are localized towards the UV brane while only the transverse gauge bosons propagate in the bulk of extra dimensions, and both the KK graviton and the radion are localized towards the IR brane. A detailed discussion on this will be given in next section.

2.2 Diphoton resonance

Suppose that diphotons come from the cascade decay of the resonance X with spin J through light intermediate particles [6–9], namely, $X \to YY \to 2\gamma_{\text{jet}}$, with $Y \to n\gamma \equiv \gamma_{\text{jet}}$ with $n = 2$ or 4, such that n photons coming from the decay of each Y are collimated and are considered as a singlet photon in the detector. In this case, the resonance production cross section of particle X with cascade decays is

$$\sigma(pp \to X \to 2\gamma_{\text{jet}}) = \frac{2J+1}{sM_X\Gamma_X} K_{gg} C_{gg} \Gamma(X \to gg)\Gamma(X \to YY)(\text{BR}(Y \to \gamma_{\text{jet}}))^2 \tag{6}$$

where the gluon luminosity is given by $C_{gg} = 2137$ for $s = (13\,\text{TeV})^2$ and the K-factor is given by $K_{gg} = 1.4$. Then, we assume that the Y couplings to gauge bosons are small enough to evade the bounds on a light scalar at the LEP or LHC but they are large enough to decay within the ECAL. In our model, we choose a KK graviton resonance of 750 GeV and a light radion, so we have $X = G$ and $Y = r$.

The hadronic decays of a light scalar with sub-GeV mass is the subject of much debate [16–18]. For $m_r < 2m_\pi \approx 280\,\text{MeV}$, the radion decays only into a photon pair in the model with suppressed lepton couplings. For $2m_\pi \approx 280\,\text{MeV} < m_r < 2m_K \approx 900\,\text{MeV}$, the radion decays mostly into a pair of pions, so the branching fraction into a photon pair is negligible. For $2m_K < m_r \lesssim 1.5\,\text{GeV}$, both $\pi\pi$ and KK decay modes are dominant. For $m_r \gtrsim 2.5\,\text{GeV}$, the description of the radion decaying into a gluon pair is well justified. However, there is a gap between $m_r = 1.5 - 2.5\,\text{GeV}$ for which neither the meson description nor the quarks/gluon description is correct, so there are large uncertainties in the hadronic decay rates [17]. In the following, we discuss the photon-jet contribution from the radion decay in each relevant case.

For $m_r < 280\,\text{MeV}$, the radion decays only into a pair of photons, of course this assumes that the light leptons are localized towards the UV brane so that their wave-function overlap with the radion is quite suppressed. Then, the decay length of the radion is estimated as

$$L = \frac{1}{\Gamma_r} \cdot \frac{E_r}{m_r} = 1.5\,\text{m}\left(\frac{0.28\,\text{GeV}}{m_r}\right)^4 \left(\frac{\Lambda/d_{\gamma\gamma}}{100\,\text{TeV}}\right)^2. \tag{7}$$

So, depending on the radion mass or $d_{\gamma\gamma}/\Lambda$, we can have a long lived radion, which is bounded by the condition that the radion decays inside ECAL for the diphoton excess. On the other hand, for $m_r > 1.5\,\text{GeV}$ including the ambiguous region for the effective description, we

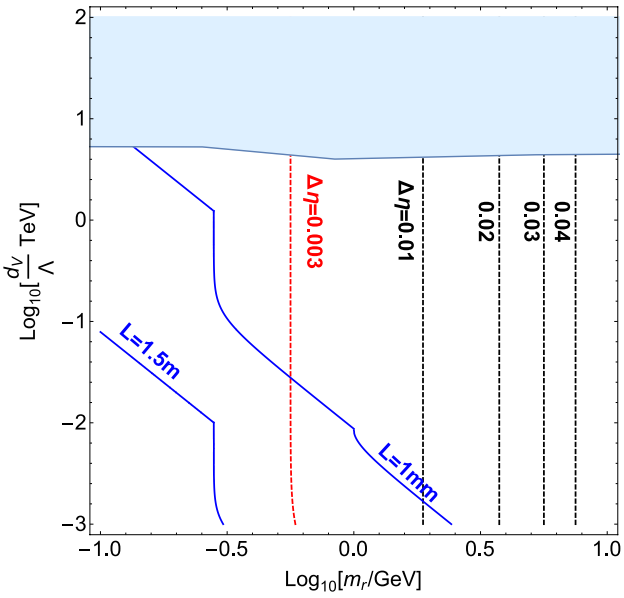

Figure 3: $\Delta\eta_{\gamma\gamma}$ between two collimated photons from the radion decay and the decay length of the radion in the parameter space, m_r vs $d_V/\Lambda[\mathrm{TeV}^{-1}]$ with $d_V \equiv d_{\gamma\gamma} = d_{gg}$. Current exclusion are adapted from the analyses in Refs. [19, 20].

include the radion decay into a gluon pair, leading to the decay length of the radion as

$$L = \frac{1}{\Gamma_r} \cdot \frac{E_r}{m_r} = 2.0 \times 10^{-4}\,\mathrm{m} \left(\frac{1.5\,\mathrm{GeV}}{m_r}\right)^4 \left(\frac{\Lambda/d_V}{100\,\mathrm{TeV}}\right)^2 . \tag{8}$$

with $d_V \equiv d_{\gamma\gamma} = d_{gg}$. Then, including both single and two-photon events from the decays of the KK graviton, the diphoton production cross section is

$$\Gamma_G(gg)[\Gamma_G(\gamma\gamma) + \Gamma_G(rr)(\mathrm{BR}(r \to \gamma\gamma))^2] = 1.24 \times 10^{-5}\mathrm{GeV}^2 \left(\frac{\sigma(pp \to \gamma\gamma)}{6\,\mathrm{fb}}\right)\left(\frac{\Gamma_G}{0.1\,\mathrm{GeV}}\right). \tag{9}$$

For $2m_\pi \approx 280\,\mathrm{MeV} < m_r < 2m_K \approx 900\,\mathrm{MeV}$, the partial decay rate of the radion decaying into a pair of pions ($\pi^a\pi^a$ with $a = 1, 2, 3$) is calculated in chiral perturbation theory as discussed in the previous section. Then, the ratio of decay rates of the pion and would-be gluon decay modes is given by $\Gamma_r(\pi^a\pi^a)/\Gamma_r(gg) = 6 - 7.5$, depending on the radion mass. Thus, for $d_{\gamma\gamma} = d_{gg}$, the radion decays mostly into a pair of pions. In this region, the decay length is estimated as follows,

$$L = \frac{1}{\Gamma_r} \cdot \frac{E_r}{m_r} \simeq 8.2 \times 10^{-4}\,\mathrm{m} \left(1 + \frac{m_\pi^2}{m_r^2}\right)^{-2} \left(1 - \frac{4m_\pi^2}{m_r^2}\right)^{-1/2} \left(\frac{0.5\,\mathrm{GeV}}{m_r}\right)^4 \left(\frac{\Lambda/d_V}{100\,\mathrm{TeV}}\right)^2 \tag{10}$$

with $d_V \equiv d_{\gamma\gamma} = d_{gg}$. In this case, the diphoton events have a photon-jet contribution, produced from the decay of neutral pions in the cascade decay of the radion. Including single and four-photon events from the decays of the KK graviton, the condition for diphoton production becomes then

$$\Gamma_G(gg)[\Gamma_G(\gamma\gamma) + \Gamma_G(rr)(\mathrm{BR}(r \to \pi^0\pi^0))^2] = 1.24 \times 10^{-5}\mathrm{GeV}^2 \left(\frac{\sigma(pp \to \gamma\gamma)}{6\,\mathrm{fb}}\right)\left(\frac{\Gamma_G}{0.1\,\mathrm{GeV}}\right). \tag{11}$$

For $m_r > 2m_{\pi^\pm}$, the branching fraction of the radion into a pair of neutral pions is about $\mathrm{BR}(r \to \pi^0\pi^0) \simeq \frac{1}{3}$. But, for $2m_{\pi^0} < m_r < 2m_{\pi^\pm}$, the radion can decay almost fully into a pair of neutral pions. In the latter case, it is possible to have a large photon-jet contribution from four photons per each radion decay.

Finally, for $2m_K < m_r < 1.5\,\mathrm{GeV}$, the radion can also decay into a pair of kaons and/or a pair of η mesons, on top of pions. The partial decay rates for these decays can be computed in a similar way to the pion decay modes, but with the inclusion of the s quark in chiral perturbation theory. For instance, the decay rate into a pair of kaons is given by eq. (5) with $b = 9$ and m_π being replaced by m_K. In this region, the decay rates of the radion into a photon-jet is further suppressed due to the presence of extra meson decay modes.

In Fig. 3, we show the separation of two collimated photons in pseudo-rapidity, $\Delta\eta_{\gamma\gamma}$, and the decay length L, in the parameter space of the effective coupling $d_V/\Lambda[\mathrm{TeV}^{-1}]$ and mass m_r of radion. In this case, the pseudo-rapidity separation can be smaller than 0.003 as required from the least cell size of the first layer in ATLAS ECAL. In the presence of the radion coupling to $Z\gamma$, we can also impose the LEP limit from $e^+e^- \to Z \to a\gamma$ with axion-like particle decaying by $a \to \gamma\gamma$ near the Z pole, as shown in gray region. In the region above the pion threshold with $m_r > 2m_\pi$, the branching fraction of $r \to \gamma\gamma$ gets suppressed so the LEP limit disappears in the figure. However, if there is no $Z\gamma$ coupling to the radion, which is the case with $d_1 = d_2$ that we will focus on in the later discussion, the LEP limit in Fig. 3 does not apply.

In Fig. 4, we show the parameter space in c_1 vs c_3 for varying radion self-coupling, c_{rr}. We took the masses of the KK graviton and the radion to 750 GeV and 0.2 GeV, respectively, so the diphoton excesses can be due to the direct or cascade decays of the KK graviton. The radion mass is small enough such that it decays fully into a pair of photons, namely, $\mathrm{BR}(r \to \gamma\gamma) = 1$. In the figures, the region satisfying the diphoton conditions (9) or (11) for $\sigma(pp \to \gamma\gamma) = 5 - 11\,\mathrm{fb}$ is shown in blue while the region consistent with LHC 8TeV data is shown in red. The region excluded by dijet searches is shown in gray. Here, for the left and middle plots in Fig. 4, we took the same ratios of effective couplings, $d_1/d_3 = c_1/c_3$, for simplicity, which is the case when the wave function overlaps are determined by those of bulk gauge fields in the minimal RS model.

Defining R as the ratio of photon-jet and single photon contributions to the diphoton bump as follows,

$$R \equiv \frac{\Gamma_G(rr)(\mathrm{BR}(r \to \gamma_{\mathrm{jet}}))^2}{\Gamma_G(\gamma\gamma)}, \tag{12}$$

with $\gamma_{\mathrm{jet}} = 2\gamma$ or 4γ, we find from the left and middle plots in Fig. 4 that the larger the decaying branching fraction $\mathrm{BR}(G \to rr)$ (or the larger c_{rr}), the wider the region with large R. In the rightmost plot in Fig. 4, we also draw the contour plots with constant R in the parameter space of $c_1 = c_2$ vs c_{rr} for $m_G = 750\,\mathrm{GeV}$ and $m_r = 0.2\,\mathrm{GeV}$. From the left plot in Fig. 4, when the coupling c_{rr} between radion and KK graviton is small, the gluon coupling can be large, even with large R. But, the larger c_{rr} gets, the smaller the gluon coupling becomes, as shown in the middle plot in Fig. 4.

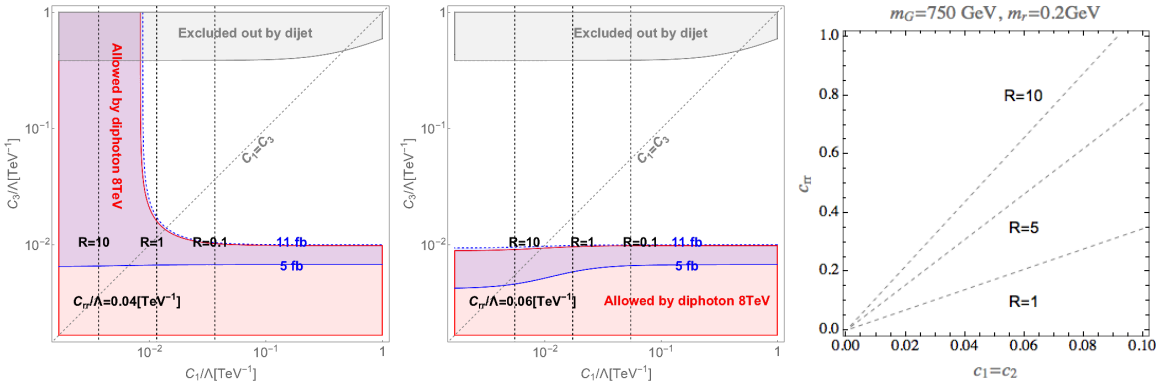

Figure 4: (Left,Middle) Parameter space of c_1 and c_3 for the diphoton resonance, depending on the radion-KK graviton coupling, $c_{rr}/\Lambda(\text{TeV}) = 0.04, 0.06$, on left and in middle, respectively. (Right) Contour plots of R values for photon-jet contribution in $c_1 = c_2$ vs c_{rr}. We took the KK graviton and radion masses to be $m_G = 750\,\text{GeV}$ and $m_r = 0.2\,\text{GeV}$ while $c_1 = c_2$, $c_H = c_f = 0$, and $d_1/d_3 = c_1/c_3$ are chosen. Several contours with constant R (defined in the text) are shown in left and middle plots. The region explaining the diphoton resonance at 750 GeV for $\sigma(pp \to \gamma\gamma) = 5 - 11\,\text{fb}$ and the region allowed by diphoton searches at CMS 8 TeV are shown in blue and red, respectively. The region excluded by dijet searches is shown in gray. The line with $c_1 = c_3$ is shown in each plot, as it is the case for minimal radion couplings to the bulk gauge fields in the bulk RS model.

3 Radion and KK graviton from warped geometry

In this section we consider a concrete model for the effective interactions of the radion and a KK graviton in the context of warped gravity, in particular, the RS framework. Then, we discuss more general cases where there appear non-universal couplings of the radion and KK graviton to the SM gauge bosons and enhanced couplings between radion and KK graviton.

3.1 Wave functions of radion and KK graviton

We identify Kaluza-Klein graviton and radion in the RS framework as CP-even spin-2 and spin-0 fields, respectively, discussed in the previous section. The corresponding 5D gravitational action is given by

$$S_5 = \int d^4x \int_0^L dy\ \sqrt{|g|} M_*^3 \left(-\mathcal{R}_5 + 12k^2\right) + \left(\sqrt{|g|} M_*^3 \left(k_B \pm \frac{1}{2k} r_{0,L} \mathcal{R}_4\right)\right)\Big|_0^L \qquad (13)$$

where M_* is a mass term which defines the 5D mass scale, k is the bulk curvature constant, and k_B determines the brane tensions which allow an AdS solution to the Einstein equations for the bulk. The 4D Einstein terms on the branes generate brane kinetic terms (BKTs) for the graviton and radion, controlled by the $r_{0,L}$ parameters. The resulting metric is that of the Randall-Sundrum model,

$$ds^2 = e^{-2ky} \eta_{\mu\nu} dx^\mu dx^\nu - dy^2. \qquad (14)$$

At $y = 0$ and $y = L$ we have the UV and IR 3-branes, and the mass scale at which the Kaluza-Klein (KK) modes appear at is approximately $ke^{-kL} = M_{KK}$.

Our primary interest is in models in which all of the SM fields are localised on the UV brane, with the exception of the SM gauge fields, which are in the bulk. Also, we want the lightest KK graviton to be at 750 GeV and the radion to have a mass of ~ 0.2 GeV. The difficulty here arises due to the mass of the lightest KK graviton. In standard RS models the prediction is that the lightest spin-2 KK mode is heavier than the lightest spin-1 mode, where the lower bounds on the latter are ~ 3 TeV. This problem can be avoided if one tunes the gravity BKTs that we have included in our action, eq. 13. However, the required values of r_L usually imply a negative effective kinetic term for the radion, and avoiding this requires additional IR dynamics [21].

Perturbing around this background we find the graviton fluctuations, associated with the 4D components of the metric, and the radion, identified with the fluctuations along the 55 component of the metric. With the above considerations in mind, the 5D wavefunctions for the radion and graviton are found to be

$$\begin{aligned} \hat{r}(x,y) &= f_r(y) r(x), \\ \hat{G}_{\mu\nu}(x,y) &= f_G^{(n)}(y) G_{\mu\nu}^{(n)}(x) \end{aligned} \tag{15}$$

where $f_r(y) \equiv \frac{1}{\sqrt{6}\Lambda_r} e^{2k(y-L)}$ with $\Lambda_r = (M_*/k)^{3/2} M_{KK}$, and

$$f_G^{(n)}(y) = \frac{e^{2ky}}{N_n} \left(J_2\left(\frac{m_n e^{ky}}{k}\right) - \beta_n(m_n) Y_2\left(\frac{m_n e^{ky}}{k}\right)\right). \tag{16}$$

Here, m_n are the KK masses of the 4D modes, β_n is an integration constant, and N_n is a constant fixed by requiring that the kinetic term is normalised,

$$\frac{1}{k}\int_0^L dy\; e^{-2ky} f_G^{(m)} f_G^{(n)} \left(k + r_L \delta(y-L)\right) = \frac{4\delta_{mn}}{M_*^3}. \tag{17}$$

The integration constant and the KK masses are fixed by the boundary conditions for the graviton on the UV and IR branes. The boundary conditions for the graviton fields can be written as

$$\begin{aligned} f_G^{(n)}(0) &= 0 \\ f_G^{(n)\prime}(L) &= \frac{r_L m_n^2}{k e^{-2kL}} f_G^{(n)}(L). \end{aligned} \tag{18}$$

We then find the integration constant to be

$$\beta_n(m_n) = \frac{J_2(m_n/k)}{Y_2(m_n/k)} \ll 1. \tag{19}$$

In the presence of the IR BKT there exists an additional light mode in the spectrum with mass,

$$m_1 \simeq \frac{2M_{KK}}{\sqrt{r_L}}, \tag{20}$$

hence using r_L we can fix the first graviton mass to be 750 GeV. As a consequence, we can make the light KK graviton lighter than KK modes of bulk gauge bosons with masses $\gtrsim M_{KK}$, although it is at the expense of the 4D Einstein terms.

3.2 Minimal couplings and diphoton in the RS model

In this section we discuss the minimal couplings of radion and KK graviton in the RS model. First, the couplings of the KK graviton to the SM fields are given by the integration over the 5D profiles of gauge fields and KK graviton,

$$\begin{aligned} c_{1,2,3} =& \frac{\Lambda}{2L}\int_0^L f_G^{(1)} dy \\ c_{f,H} =& \frac{\Lambda}{2}\int_0^L f_{f,H}^2 f_G^{(1)} dy, \end{aligned} \tag{21}$$

where $f_{f,H}$ denotes the 5D profile of the fermion with $f = (q, tR, bR)$ or Higgs field. The 5D profiles of bulk SM fields can be written in a compact form,

$$f_a = \sqrt{\frac{2ak}{1-e^{-2akL}}} e^{-2aky} \tag{22}$$

such that they are normalised according to $\int_0^L dy f_a^2 = 1$ and $a = (a_H, a_q, a_{tR}, a_{bR})$ represents the localisation of the 5D fields. The couplings of the radion to the transverse gauge fields are,

$$d_i = \frac{\Lambda}{\Lambda_r\sqrt{6}}\left(\frac{1}{4kL} + \frac{\alpha_i}{8\pi}(b_i + F_i)\right), \quad i = 1,2,3 \tag{23}$$

where b_i are the beta function coefficients of the light fields localized on the IR brane, and F_i are loop functions coming from the couplings to heavy fields such as W and top quark [13]. If we have the Higgs and fermions on the UV brane, thus only having the gauge fields, KK gravitons, and radion in the bulk, then coupling of the KK graviton to the Higgs and fermions is negligible compared to the coupling to the transverse gauge fields. In addition to this, with a radion of mass ~ 0.2 GeV and the KK graviton at 750 GeV, the only relevant decay channels are $G \to VV$, $G \to rr$, and $r \to VV$. If we were to have the Higgs and some fermions localised near the IR then the situation would change drastically. The KK graviton would then have large branching fractions to the Higgs, the IR localised fermions, and the longitudinal components of $W^\pm$ and Z.

The triple coupling between the KK graviton and two radions is also similarly given by the integration over the 5D profiles of KK graviton and radion as

$$c_{rr} = \frac{\Lambda}{3\Lambda_r^2}\int_0^L dy\; e^{2k(y-2L)} f_G^{(1)} \simeq \frac{\Lambda}{3N_1\Lambda_r^2}\int_0^L dy\; e^{4k(y-L)} J_2\left(\frac{m_1 e^{ky}}{k}\right), \tag{24}$$

where the last expression naively assumes that there are no gravity BKTs. Assuming that $m_r \ll m_G^{(1)}$, the above couplings should be the most relevant graviton self-interaction. There is a possibility that an off-shell graviton could be produced and radiate off a light radion too. The triple coupling between KK graviton and two radions [3] stem from the graviton self-interactions of the 5D Einstein term and it is given by $c_{rr} \sim 0.1$, which is sizable due to the simultaneous localization of both KK graviton and radion toward the IR brane. Therefore, we can make use of such a sizable coupling for explaining the diphoton excess in terms of the

[3] There is a triple coupling between two KK gravitons and one radion too, as shown in the appendix, but it is not relevant for our discussion on the diphoton resonance.

cascade decay of the KK graviton into a pair of radions, with each radion decaying into a pair of photons.

Strictly speaking, one should also include the non-minimal $\xi\mathcal{R}H^\dagger H$ coupling in our discussion, which induces a mixing between the radion and the Higgs as well as additional BKT terms for the radion and graviton [13, 15]. If the Higgs is localised on the UV brane, this coupling will be very suppressed due to the small overlap between the Higgs and the radion. With an IR localised Higgs the effect could be large, however it is interesting to note that in the scenario where the Higgs arises as a Goldstone boson, the non-minimal coupling cannot be induced at tree-level, and is expected to be small [31]. In our work we will neglect this Higgs-radion mixing.

In the simplest KK graviton case, without graviton BKTs and with the SM gauge fields on the IR brane, the gauge boson couplings to the 1st KK graviton are $c_i \sim (kL)^{-1} = [\ln(\Lambda_{\rm UV}/\Lambda)]^{-1} \sim 0.03$ with an IR scale of $\Lambda \sim 1\,\text{TeV}$ and a UV scale of $\Lambda_{UV} = M_P$. And at the same time, ignoring trace anomalies and loop corrections, we obtain the gauge boson couplings of the radion as $d_i \sim (kL)^{-1}/(4\sqrt{6}) = [4\sqrt{6}\ln(\Lambda_{\rm UV}/\Lambda)]^{-1} \sim 0.003$. Therefore, in the minimal setup, the radion couplings to gauge bosons are much suppressed as compared to those of the KK graviton. The minimal couplings of radion and KK graviton in RS model (without gravity BKTs, i.e. $r_L = 0$) are summarized in Table 1.

	VV	rr	GG
radion	$0.003\,(35/(kL))$	-	0.2
KK graviton	$0.03\,(35/(kL))$	0.1	-

Table 1: Minimal couplings of radion and KK graviton in RS model as a function of the volume factor, kL.

Using the couplings from table 1, the partial decay rates of the KK graviton with $m_G = 750\,\text{GeV}$ are

$$\Gamma_G(gg) = \frac{c_{gg}^2 m_G^3}{10\pi\Lambda^2} = 0.012\ \text{GeV}\Big(\frac{1\,\text{TeV}}{\Lambda}\Big)^2\Big(\frac{35}{kL}\Big)^2, \tag{25}$$

$$\Gamma_G(\gamma\gamma) = \frac{c_{\gamma\gamma}^2 m_G^3}{80\pi\Lambda^2} = 0.0015\ \text{GeV}\Big(\frac{1\,\text{TeV}}{\Lambda}\Big)^2\Big(\frac{35}{kL}\Big)^2, \tag{26}$$

$$\Gamma_G(rr) = \frac{c_{rr}^2 m_G^3}{960\pi\Lambda^2}\Big(1 - \frac{4m_r^2}{m_G^2}\Big)^{5/2} = 0.0014\ \text{GeV}\Big(\frac{1\,\text{TeV}}{\Lambda}\Big)^2. \tag{27}$$

Thus, the KK graviton decays dominantly into a pair of gluons while the decay rate of the KK graviton into a pair of radions is comparable to the one into a photon pair. On the other hand, for minimal couplings of the radion with $m_r < 2m_\pi \approx 280\,\text{MeV}$, the radion decays fully into a pair of photons with the corresponding decay rate,

$$\Gamma_r(\gamma\gamma) = \frac{d_{\gamma\gamma}^2 m_r^3}{4\pi\Lambda^2} < 8.95\times10^{-14}\ \text{GeV}\Big(\frac{1\,\text{TeV}}{\Lambda}\Big)^2\Big(\frac{35}{kL}\Big)^2. \tag{28}$$

Then, the would-be photon-jet contribution to the diphoton cross section, $R = \Gamma_G(rr)/\Gamma_G(\gamma\gamma) = 0.93(kL/35)^2$. However, in order for the radion to decay inside the ECAL, we would need $kL \lesssim 11$, which implies that the UV scale must be $\Lambda_{\rm UV} \lesssim 6\times10^7\,\text{GeV}$ for $\Lambda = 1\,\text{TeV}$.

Nonetheless, for $kL \lesssim 11$, the KK graviton couplings would increase to $c_i \gtrsim 0.1$, so the R-ratio gets a smaller value, $R \lesssim 0.1$. Therefore, the minimal RS model with light radion could not give rise to significant photon-jet signals. In this case, the single photon contribution from the direct decay of the KK graviton can explain most of the diphoton excesses, as shown in Ref. [4].

Before ending this subsection, we remark on the effect of gravity BKTs on KK graviton couplings. In order to make the KK graviton of 750 GeV compatible with a heavy lightest spin-1 KK state $\gtrsim 3$ TeV as inferred from flavor violation, we require non-zero gravity BKTs. In this case, we find that the graviton couplings both to the transverse gauge fields and to the radion get suppressed, however, both couplings get suppressed by the same amount. Thus, the above conclusion on the single photon and photon-jet contributions still hold. But, as will be discussed in next section, the photon-jet contribution can be dominant in the presence of extra BKTs for gauge fields, which reduce the KK graviton couplings to gauge fields.

3.3 Beyond the minimal couplings

In this section, we show that the couplings of the KK graviton to the gauge fields can made suppressed in the presence of BKTs for gauge fields, while the radion couplings to them remain due to the classical scale invariance of those BKTs. Then, since both the KK graviton and radion couplings to the gauge fields are proportional to the inverse volume of the warped extra dimension, $(kL)^{-1}$, we can take a smaller kL in the little RS model to enlarge the radion couplings while maintaining or reducing the KK graviton couplings at the expense of gauge BKTs. In this case, the radion can decay within ECAL without affecting the ratio R for the photon-jet contribution found in the minimal model in the previous section. Therefore, the photon-jet scenario is valid due to the non-minimal couplings. We also discuss the effects of gauge BKTs on the non-universal couplings of the KK graviton as well as the lightest KK masses of gauge fields.

Consider the following action for a bulk gauge field in a warped geometry with a BKT,

$$S = -\frac{1}{4}\int d^4x \int_0^L \sum_{a=1}^{3} \Big(1 + \sigma_a \delta(y-L)\Big) F^{a,\mu\nu} F^a_{\mu\nu}, \tag{29}$$

where we do not introduce a BKT for the $\mu 5$ components of the field strength tensor, thus ignore them here. The BKTs, σ_a, are dimensionful, and modify the normalisations of the zero mode wave functions such that,

$$A_{a,\mu}(x,y) = \frac{A^0_{a,\mu}(x)}{\sqrt{L+\sigma_a}} + \dots . \tag{30}$$

By inspecting the interactions of the gauge fields we see that the relation between the 5D and effective gauge couplings in turn gets modified,

$$(g^a_5)^2 = (g^a_4)^2 (L + \sigma_a). \tag{31}$$

Since we fix g^a_4, this parameter modifies the couplings of localised fields which couple via g^a_5, i.e. KK modes. The couplings of the KK graviton and the radion get modified by this BKT in two ways; one being through the normalisation of the gauge field, and the other being due

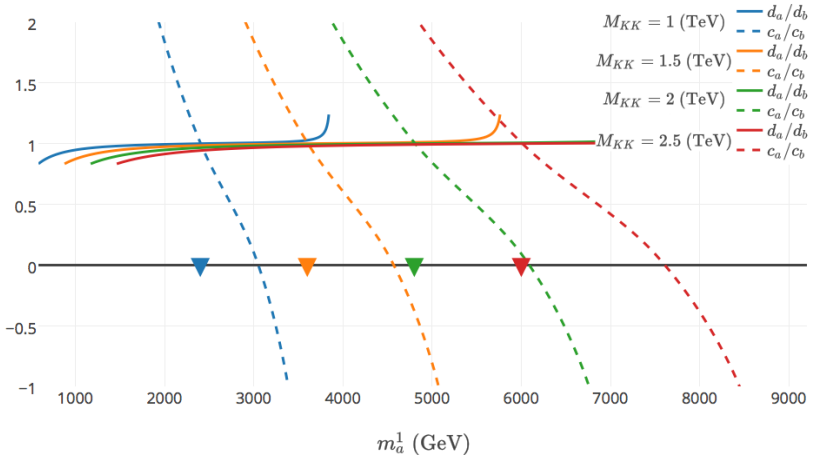

Figure 5: Here we plot the effects of gauge BKTs on the couplings of the gauge fields to a 750 GeV KK graviton and a radion, and the triangles denote the masses of the first A_μ^a mode when the BKT is zero. The BKT for A_μ^a is varied over $-0.2L < \sigma_a < 0.2L$ and the BKT for A_μ^b is kept zero. Note that to keep the results general, we have ignored the effects of the anomalous terms.

to the direct coupling of the KK graviton to the BKT. In these warped models we find that the dimensionless couplings for the KK graviton in the effective theory are given by,

$$\frac{c_a}{\Lambda} = \frac{1}{2}\frac{1}{\sqrt{L+\sigma_a}}\int_0^L (1+\sigma_a\delta(y-L))f_G^{(1)} \tag{32}$$

and the dimensionless couplings of the radion are given by,

$$\frac{d_a}{\Lambda} = \frac{(k/M_*)^{3/2}}{\sqrt{6}M_{KK}}\left(\frac{1}{4k(L+\sigma_a)} + \frac{\alpha_a}{8\pi}(b_a+F_a)\right). \tag{33}$$

As well as modifying the couplings of the gauge fields, the BKTs also modify the mass spectrum of the spin-1 modes, in fact the zero mode remains in the spectrum and the lightest massive mode is given by,

$$m_{A^a}^1 \simeq 2M_{KK}\sqrt{\frac{kL+\sigma_a k}{kL-1+2\sigma_a k^2 L-\sigma_a k}}. \tag{34}$$

If the BKTs become too large we would inevitably have light spin-1 fields in the spectrum which may be in tension with experimental bounds.

In Fig. 5, to quantify the effects of these BKTs, we plot ratios of couplings (c_a/c_b and d_a/d_b) to different gauge fields (A_μ^a and A_μ^b) where we add a BKT (σ_a) for the A_μ^a gauge field. To make this analysis general, we neglect the anomalous contributions to the radion couplings.

From Fig. 5 we see that one can completely suppress the graviton coupling to the transverse gauge fields, while the radion coupling to transverse gauge fields remains mostly unaffected. This requires a small negative BKT for the bulk gauge fields, and actually increases the mass

of the lightest KK mode. This is interesting, as we can now suppress the graviton coupling to photons while at the same time increasing the lightest KK photon mass, therefore the dominant di-photon signal can come from the photon-jets via radions. How large the photon-jet contribution is only depends on how much we are willing to tune the BKT. Note that we have checked that the negative BKTs do not lead to large changes in the effective kinetic terms for the gauge fields, the effect on the KK graviton coupling is larger due to its IR localisation.

3.4 The Composite Higgs scenario: Higgs and top in the IR

Up until now we have focused on the scenario with the Higgs and fermions on the UV brane. In this section, however, we study the photon-jet signal in the Composite Higgs scenario. In this case the Higgs field arises as A_5 components of a bulk gauge field, which are localised in the IR ($a_h = -1$), the right-handed top quark is required to be localised in the IR also ($a_{tR} = -1$), and the (t_L, b_L) doublet is required to be delocalised ($a_q \sim 0$). This model is much different than that considered previously, and the experimental bounds from Run 1 are much more stringent due to the large coupling of the KK graviton to the Higgs. It is actually the constraints from the vector boson channels which are now most constraining, as the KK graviton has a large coupling to the longitudinal components of these fields via the Higgs.

To remain within the experimental constraints we employ the same mechanism used in [28], in which the authors lower the 5D volume of the extra dimension, $\Omega = k/M_{KK}$, in order to enhance the KK graviton coupling to the transverse gauge fields. In this work it was shown that a value of $k \sim 10^3$ TeV (with $M_{KK} = 1.2$ TeV) was required in order sufficiently enhance the decays of the KK graviton to photons, while remaining within run 1 bounds, however the presence of the radion was ignored. In this analysis we will not only include a light radion and study the photon-jet signal arising from the cascade decay, but we will also investigate what happens when we turn on the hypercharge BKT.

We have to look at $\Gamma(X \to ff)/\Gamma(X \to \gamma\gamma)$ (with ff some final state) to determine whether or not these predictions are in contradiction with existing bounds from Run 1 and 2 LHC data. The current upper bounds on these ratios are [22–27], as shown in Table 2.

	ZZ	WW	$Z\gamma$	hh	$t\bar{t}$
$R_{ff} = \frac{\Gamma(X\to ff)}{\Gamma(X\to\gamma\gamma)}$	10	40	6	40	400

Table 2: LHC bounds on the decay rates of the diphoton resonance.

In Fig. 6 we choose $M_{KK} = 1.2$ TeV, keeping hypercharge BKT at zero for now, and plot all channels for the KK graviton. We see that the ZZ channel is the most constraining and implies an upper bound on $\log(\Omega)$ of ~ 3. At this point the photon-jet contribution to the di-photon signal can be seen to be $\sim 20\%$. As we vary $\log(\Omega)$, the di-photon cross-section changes, however we then vary M_* to correct for this change keeping the di-photon cross-section constant throughout.

Even when we turn on the hypercharge BKT we find that the ZZ channel is always the most constraining. Thus in Fig. 7 we plot something similar to figure 6 but only for the ZZ channel and the ratio R. However this time we turn on the hypercharge BKT. As expected, with a hypercharge BKT the upper bound on $\log(\Omega)$ increases due to the BKT contribution

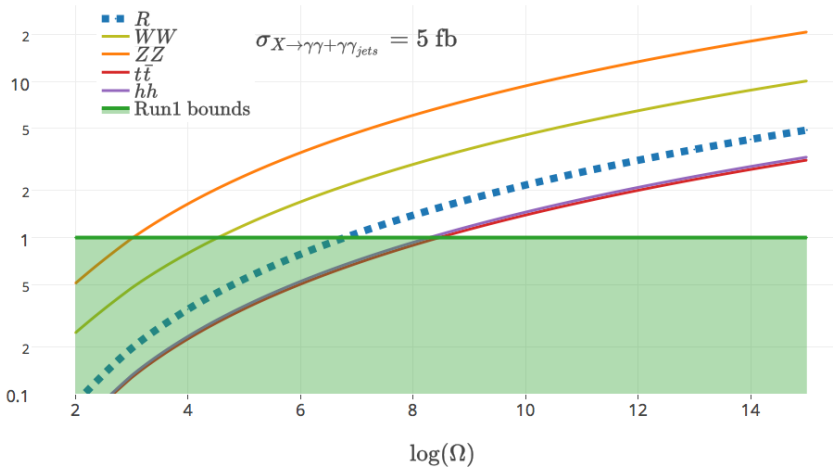

Figure 6: Here we plot the branching ratios of the 750 GeV KK graviton into different channels divided by the bounds on this channel from Run1 constraints when $M_{KK} = 1.2$ TeV and the hypercharge BKT is zero. The blue dashed line corresponds to the ratio between the photon-jet contribution and the di-photon contribution to the signal.

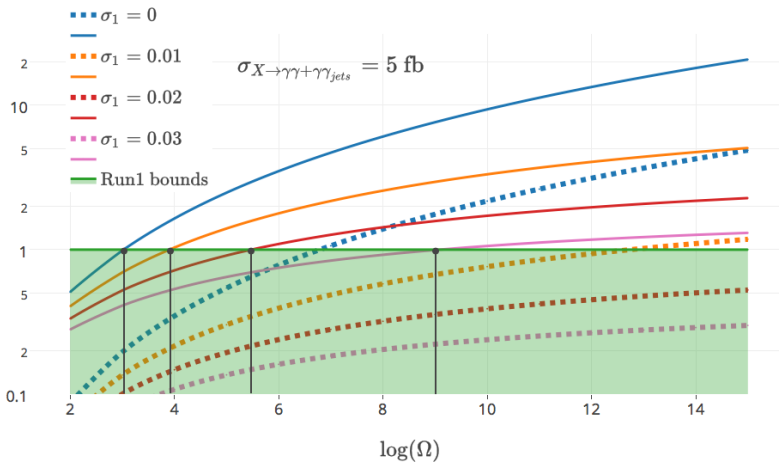

Figure 7: Considering that the ZZ channel is the most constraining in this class of models, we plot the branching ratios of the 750 GeV KK graviton into this channel divided by the Run1 bounds (solid lines). We have set $M_{KK} = 1.2$ TeV and varied the hypercharge BKT. The dashed lines corresponds to the ratio between the photon-jet contribution and the di-photon contribution to the signal.

to the KK graviton coupling to the hypercharge boson. But we also see that this does not increase the photon-jet contribution to the di-photon signal. In fact, as long as we are within run 1 bounds, the maximum contribution of photon-jets, irrespective of the hypercharge BKT, seems to be $\sim 20\%$.

The reason for this is quite obvious, the radion and the A_5 Higgs mode have the same localisation. Thus c_h/c_{rr} will remain constant as we alter $\log(\Omega)$ and M_*. Since the most stringent bounds come from the coupling of the KK graviton to the longitudinal gauge components, they essentially give an upper bound for c_h, thus they also give an upper bound for c_{rr}.

4 Phenomenology of photon-jets

In this section, we discuss the possibility of distinguishing the photon-jet contribution in our model from the single photon contribution by converted photons. Moreover, we also show that the angular distributions of photons can be used to infer the information of direct or cascade decays of the KK graviton, in comparison to the direct decay of a spin-0 resonance.

4.1 Converted photons

A photon candidate is reconstructed from the energy deposited in the ECAL after different shape variables of energy profiles are imposed. For instance, the ATLAS ECAL consists of three layers. The first layer is segmented into high granularity strips with $\Delta\eta = 0.003$-0.006 depending on η, with which we are able to make the γ-π^0 discrimination. The second layer of the ECAL has a granularity of 0.025×0.025 in $\Delta\eta\times\Delta\phi$ (corresponding to one cell). Generally if a bunch of highly collinear photons ("photon-jets") are contained in a very small cone with $\Delta R \lesssim 0.003$, the photon bunch could possibly pass the photon selection and be taken as a single photon[4].

In our model, depending on the radion mass and couplings, the diphoton signal could come from two photons or one photon + one photon-jet or two photon-jets. Even the case of two photon-jets could be divided into two categories: one category is that the photon-jet contains two photons coming from the direct decay of the radion and the other category is that the photon-jet contains four photons coming from the cascade decay of the radion into $2\pi^0$. Therefore, it is very crucial to identify the contribution of photon-jets events from the diphoton events for extracting the model parameters.

In addition to the energy deposition from the ECAL, a photon could be converted into electron and positron pair while traveling in the inner detector, resulting in a photon candidate with tracks. Thus, the photon candidates with tracks are taken as "converted" photons, and are otherwise taken as "unconverted" photons. The photon conversion rate is well studied from experiment and it varies from 0.2 to 0.4 depending on η and p_T of the photon [34]. Since photon-jets contain more than one photon, the conversion rate is expected to be larger than that of a single photon. Therefore, the number of "converted" and "unconverted" photons could provide information on the origin of the diphoton signal.

[4] A dedicated simulation is needed to show the exact percentage of faked photons coming from photon-jets.

There have already been some studies on distinguishing the photon-jets from a single photon by using the number of "converted" photons as well as the energy deposition in the ECAL [6, 8, 35]. In Ref. [35], it was shown that the substructure variables could help to discriminate photon-jets from single photon if the separation of photons inside the photon-jets is large enough ($\Delta R \sim 0.01$). A more dedicated analysis on the 750 GeV excess is performed in Ref. [8] from the counting of the number of "converted" photons. They provided the required number of events to distinguish between the case where the 750 GeV excess is solely from photon-jets, one genuine photon per photon-jet, and the case where the 750 GeV excess is from two single photons. In Ref. [6], the energy deposition of two photons is utilized. All the previous methods must be confirmed by experimentalists and especially, more information about the number of "converted" photons is necessary before any conclusion is drawn.

4.2 Angular distributions

When two photons (or a fake photon, in our case, a photon-jet) is produced from the decay of a heavy resonance (X) at the LHC, we can determine the properties of X only by the phase space variable, $\cos\theta^*$, the scattering angle of a photon relative to the beam axis at the rest frame of X. In the case where X is a KK graviton (G), the differential cross section with respect to $\cos\theta^*$ depends on the initial parton states for the production of G [29]. In the case of the diphoton resonance, the gluon initial states ($gg \to X$) are favoured, as the luminosity increase in PDF at 13 TeV makes the diphoton resonance compatible with the 8 TeV data. The corresponding angular distributions of the two-photon channel would be

$$\frac{\mathrm{d}\hat{\sigma}}{\mathrm{d}\cos\theta^*} \propto \begin{cases} 1 + 6\cos^2\theta^* + \cos^4\theta^* & \text{in } (gg \to G \to \gamma\gamma), \\ 1 - 2\cos^2\theta^* + \cos^4\theta^* & \text{in } (gg \to G \to r\,r \to 2\gamma_{\text{jet}}), \\ 1 & \text{in } (gg \to S \to \gamma\gamma), \end{cases} \tag{35}$$

with X being a spin-2 KK graviton in the first two lines and, for comparison, a scalar particle (S) in the last line. In order to make a precise determination of the particles properties using the angular variable, we require more statistics than for the discovery [30]. But the different kinematical behavior also affects the efficiencies of the analysis cuts, the rapidity coverage of the detector geometry, for example. From the simple relation between $\cos\theta^*$ and the rapidity η, we rewrite the angular distributions in the following way,

$$\frac{\mathrm{d}\hat{\sigma}}{\mathrm{d}\eta^*} \propto \begin{cases} \cosh(4\eta^*)\,\mathrm{sech}^6\,\eta^* & \text{in } (gg \to G \to \gamma\gamma), \\ \mathrm{sech}^6\,\eta^* & \text{in } (gg \to G \to r\,r \to 2\gamma_{\text{jet}}), \\ \mathrm{sech}^2\,\eta^* & \text{in } (gg \to S \to \gamma\gamma). \end{cases} \tag{36}$$

Here we use η^* to denote the rest frame, or center of mass frame, of X.

In Fig. 8, we have shown the distributions of photons as a function of the scattering angle $\cos\theta^*$ in (a) and the pseudo-rapidity η^* in (b) in the Center of Mass (CM) frame of the KK graviton. After the PDF convolution, the differential distributions of η in the LAB frame can be obtained from the above η^* distributions. To see the effect of gluon PDFs, we performed a parton-level Monte Carlo simulation as shown in Fig. (8) with Madgraph [33]. As a result, in the case where a light radion induces fake photons, many of the events would be in the

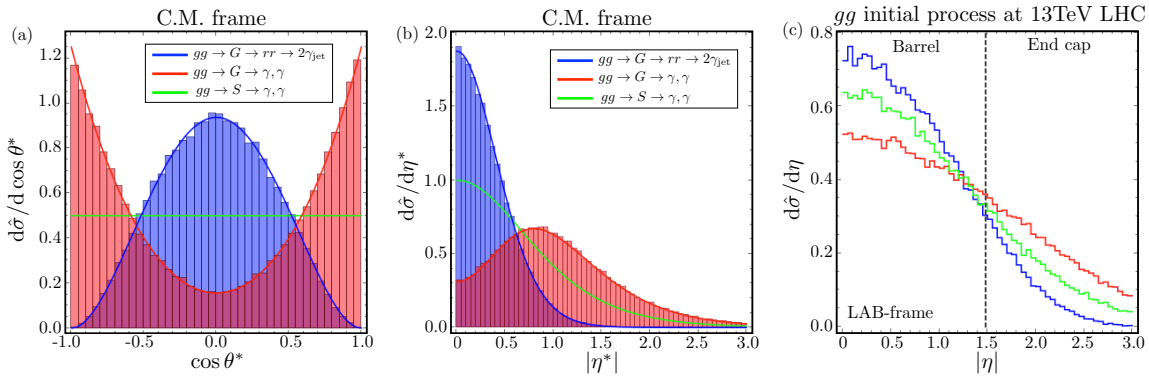

Figure 8: (a) Distributions of photons for the scattering angle $\cos\theta^*$, (b) pseudo-rapidity η^* in the CM frame of the KK graviton and (c) η at the LAB frame. Red lines correspond to $G \to \gamma\gamma$ while blue lines correspond to $G \to rr \to 2\gamma_{\rm jet}$ with $\gamma_{\rm jet}$ as a photon-jet. For comparison, we add the case for a spin-0 resonance with $S \to \gamma\gamma$ in green lines.

central(Barrel) region of the detector. In the case with the direct decay of a KK graviton, more than 30% events would be in the end cap region as in Fig. 8-(c). In our case with photon-jets, however, only about 15% events would be in the End-cap region. The results can be compared to the case of a scalar particle where 25% events would be in the End-cap region. Therefore, the optimized search for the cascade decays in our model ($G \to rr \to 2\gamma_{\rm jet}$) would be closer to the case for spin-0 resonance rather than the case for spin-2 resonance with direct decays, due to the population of events in the central region of the detector.

5 Radion and KK graviton as mediators of dark matter

Suppose that dark matter is localized toward the IR brane. In this case, both the KK graviton and the radion can have sizeable couplings to dark matter so that they can mediate between dark matter and the SM particles [4, 14]. Given that the radion is sub-GeV, the radion mediated channels give dominant contributions to the total annihilation cross section of dark matter, away from the resonance with KK graviton exchanges.

The effective interactions of KK graviton and radion to dark matter are given by

$$\mathcal{L}_{\rm KK} = -\frac{1}{\Lambda} G^{\mu\nu} T^{\rm DM}_{\mu\nu} + \frac{1}{\sqrt{6}\Lambda}\, r\, T^{\rm DM}, \tag{37}$$

where the energy-momentum tensor for dark matter, depending on the spin $(0, 1/2, 1)$ of dark

matter, is given by

$$
\begin{aligned}
T^{\rm S}_{\mu\nu} &= c_S\left[\partial_\mu S\partial_\nu S-\frac{1}{2}g_{\mu\nu}\partial^\rho S\partial_\rho S+\frac{1}{2}g_{\mu\nu}m_S^2S^2\right], &(38)\\
T^{\rm F}_{\mu\nu} &= c_\chi\left[\frac{i}{4}\bar\chi(\gamma_\mu\partial_\nu+\gamma_\nu\partial_\mu)\chi-\frac{i}{4}(\partial_\mu\bar\chi\gamma_\nu+\partial_\nu\bar\chi\gamma_\mu)\chi-g_{\mu\nu}(i\bar\chi\gamma^\mu\partial_\mu\chi-m_\chi\bar\chi\chi)\right]\\
&\quad+\frac{i}{2}g_{\mu\nu}\partial^\rho(\bar\chi\gamma_\rho\chi)\Big],\\
T^{\rm V}_{\mu\nu} &= c_X\left[\frac{1}{4}g_{\mu\nu}X^{\lambda\rho}X_{\lambda\rho}+X_{\mu\lambda}X^\lambda{}_\nu+m_X^2\Big(X_\mu X_\nu-\frac{1}{2}g_{\mu\nu}X^\lambda X_\lambda\Big)\right]. &(39)
\end{aligned}
$$

Here we note that the couplings of the KK graviton and the radion to dark matter can be different, so $c_{S,\chi,X}$ should be replaced by $c^G_{S,\chi,X}$ and $c^r_{S,\chi,X}$ for the KK graviton and radion couplings, respectively. In the presence of the couplings between the KK graviton and dark matter, the KK graviton could decay invisibly into a pair of dark matter particles, if kinematically allowed. The corresponding partial decay rates of the invisible decays are

$$
\begin{aligned}
\Gamma(SS) &= \frac{(c^G_S)^2m_G^3}{960\pi\Lambda^2}\Big(1-\frac{4m_S^2}{m_G^2}\Big)^{\frac{5}{2}}, &(40)\\
\Gamma(\chi\bar\chi) &= \frac{(c^G_\chi)^2m_G^3}{160\pi\Lambda^2}\left(1-\frac{4m_\chi^2}{m_G^2}\right)^{\frac{3}{2}}\left(1+\frac{8}{3}\frac{m_\chi^2}{m_G^2}\right), &(41)\\
\Gamma(XX) &= \frac{(c^G_X)^2m_G^3}{960\pi\Lambda^2}\Big(1-\frac{4m_X^2}{m_G^2}\Big)^{\frac{1}{2}}\Big(13+\frac{56m_X^2}{m_G^2}+\frac{48m_X^4}{m_G^4}\Big). &(42)
\end{aligned}
$$

Due to dilatation symmetry, the non-derivative couplings of radion are fixed beyond the linear order [14] as

$$
\begin{aligned}
\mathcal{L}_{\rm non-deriv} &= 2\Big(\frac{r}{\sqrt{6}\Lambda}-\frac{r^2}{3\Lambda^2}\Big)c^r_Sm_S^2S^2+\frac{r}{\sqrt{6}\Lambda}c^r_\chi m_\chi\bar\chi\chi\\
&\quad-\Big(\frac{r}{\sqrt{6}\Lambda}-\frac{r^2}{6\Lambda^2}\Big)c^r_Xm_X^2X_\mu X^\mu. &(43)
\end{aligned}
$$

For illustration purposes, in the following discussion we focus on Dirac fermion dark matter with a radion mediator and consider the radion couplings to transverse gauge bosons and a KK graviton only, i.e. with $d_H=d_V=d_f=0$. Then, the partial annihilation cross sections

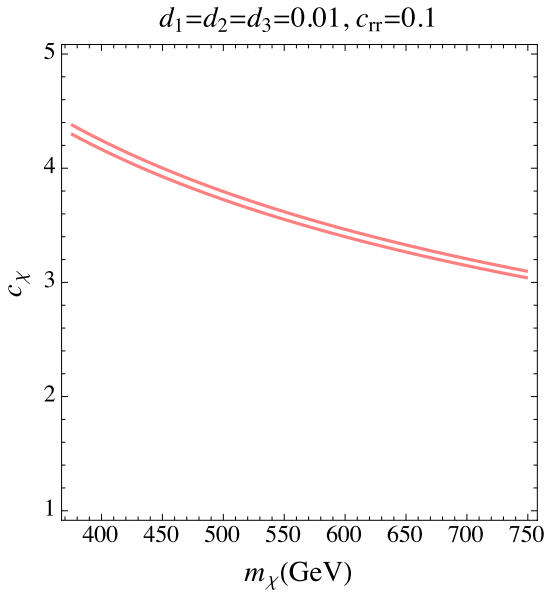

Figure 9: Parameter space for dark matter mass (m_χ) and radion coupling to dark matter (c_χ^r), satisfying the relic density given by Planck within 3σ. We have taken $\Lambda = 1\,\text{TeV}$, $d_1 = d_2 = d_3 = 0.01$ and $c_{rr} = 0.1$.

into a pair of SM gauge bosons are given [9] by

$$(\sigma v_{\rm rel})_{gg} = \frac{4(c_\chi^r)^2 d_{gg}^2}{3\pi\Lambda^4}\,\frac{m_\chi^6}{(4m_\chi^2-m_r^2)^2+\Gamma_r^2 m_r^2}\,v_{\rm rel}^2, \tag{44}$$

$$(\sigma v_{\rm rel})_{\gamma\gamma} = \frac{(c_\chi^r)^2 d_{\gamma\gamma}^2}{6\pi\Lambda^4}\,\frac{m_\chi^6}{(4m_\chi^2-m_r^2)^2+\Gamma_r^2 m_r^2}\,v_{\rm rel}^2, \tag{45}$$

$$(\sigma v_{\rm rel})_{Z\gamma} = \frac{(c_\chi^r)^2 d_{Z\gamma}^2}{12\pi\Lambda^4}\,\frac{m_\chi^6}{(4m_\chi^2-m_r^2)^2+\Gamma_r^2 m_r^2}\left(1-\frac{m_Z^2}{4m_\chi^2}\right)^3 v_{\rm rel}^2, \tag{46}$$

$$(\sigma v_{\rm rel})_{ZZ} = \frac{(c_\chi^r)^2 d_{ZZ}^2}{6\pi\Lambda^4}\,\frac{m_\chi^6 v_{\rm rel}^2}{(4m_\chi^2-m_r^2)^2+\Gamma_r^2 m_r^2}\left(1-\frac{m_Z^2}{m_\chi^2}+\frac{3m_Z^4}{8m_\chi^4}\right)\left(1-\frac{m_Z^2}{m_\chi^2}\right)^{1/2}, \tag{47}$$

$$(\sigma v_{\rm rel})_{WW} = \frac{(c_\chi^r)^2 d_{WW}^2}{12\pi\Lambda^4}\,\frac{m_\chi^6 v_{\rm rel}^2}{(4m_\chi^2-m_r^2)^2+\Gamma_r^2 m_r^2}\left(1-\frac{m_W^2}{m_\chi^2}+\frac{3m_W^4}{8m_\chi^4}\right)\left(1-\frac{m_W^2}{m_\chi^2}\right)^{1/2} \tag{48}$$

where $d_{\gamma\gamma} = s_\theta^2 d_2 + c_\theta^2 d_1$, $d_{ZZ} = c_\theta^2 d_2 + s_\theta^2 d_1$, $d_{Z\gamma} = s_\theta c_\theta (d_2 - d_1)$, $d_{gg} = d_3$, $d_{WW} = 2d_2$, We note that all the gauge boson channels are p-wave suppressed. Furthermore, for $m_\chi > m_r$, dark matter can annihilate into a pair of radions. In the limit of non-relativistic dark matter, the corresponding annihilation cross section for the rr channel [9] becomes

$$(\sigma v_{\rm rel})_{rr} = \frac{(c_\chi^r)^4}{288\pi\Lambda^4}\,\frac{m_\chi^6(2(m_r^2-2m_\chi^2)^2+m_\chi^4)}{3(m_r^2-2m_\chi^2)^4}\left(1-\frac{m_r^2}{m_\chi^2}\right)^{1/2} v_{\rm rel}^2\,. \tag{49}$$

Thus, the rr channel turns out to be also p-wave suppressed, but it can contribute to the thermal cross section at freeze-out. If $m_\chi > (m_G + m_r)/2$, the rG channel would be open too

and the corresponding annihilation cross section is given by

$$(\sigma v_{\rm rel})_{Gr} = \frac{(c_\chi^r)^2 c_{rr}^2}{9\pi\Lambda^4} \frac{m_\chi^{10} v_{\rm rel}^2}{((4m_\chi^2 - m_r^2)^2 + \Gamma_r^2 m_r^2) m_G^4} \left(1 - \frac{(m_G - m_r)^2}{4m_\chi^2}\right)^{5/2} \left(1 - \frac{(m_G + m_r)^2}{4m_\chi^2}\right)^{5/2}. \quad (50)$$

We note that the KK graviton mediator also contributes to the annihilation of the above fermion dark matter too, becoming important near the resonance region. But, we ignore the contributions from the KK graviton, focusing on the region outside the resonance.

In Fig. 9, we show the parameter space for the dark matter mass and coupling to the radion, considering the bound on the relic density from Planck within 3σ. We took the radion couplings to the SM gauge bosons and to the KK graviton such that the photon-jet contribution to the diphoton excess is dominant. Therefore, a sizable radion coupling to dark matter can accommodate a correct relic density. For $m_\chi < m_G/2 = 375\,\text{GeV}$, there would be an invisible decay of the KK graviton into a pair of dark matter. If the KK coupling is of a similar order to the radion counterpart (namely, $c_\chi^G \sim c_\chi^r$), the invisible decay would be too large for the branching fractions of KK graviton decaying into $\gamma\gamma$ or rr to accommodate the diphoton excesses. Thus, we took $m_\chi > 375\,\text{GeV}$ in Fig. 9. But, if the KK graviton coupling to dark matter gets smaller, the invisible decay rate of the KK graviton could be at the level of detectability in the near future at the LHC [4].

6 Conclusions

We have presented a theoretical framework to study the diphoton excess as a manifestation of the interplay between direct decays to photons or photon-jets, originating from the sequential decay of the 750 GeV resonance to a pair of new light resonances. We assumed the new resonances are spin-two and -zero particles (decaying in that order) motivated by theories of warped gravity at the TeV scale, and explored the phenomenology in the model-independent fashion.

We showed that a large wavefunction overlap between the KK graviton and the radion in the warped extra dimension allows for a large gravity self-coupling between them in 4D effective theory, making the KK graviton decay largely into a pair of radions. As a light radion can decay mostly into a pair of photons, the resulting photon-jets from the decay of the KK graviton can mimick the diphoton excesses due to the limited η resolution of single photons in the ECAL. We provided an explicit realization of the photon-jet scenario in the extra dimension, being consistent with current limits from direct searches and electroweak tests.

We found that angular distributions of the two jets could be a handle to distinguish between direct photon and photon-jet situations in our model. For instance, the direct photons are more directed towards the End-cap region while the photon-jets are more directed towards the central(Barrel) region. Furthermore, photon-jets in our model turn out to be more central than single photons obtained from the direct decay of a spin-0 resonance.

New resonances such as a KK graviton and a radion can play the role of the mediator of dark matter and could be seen from the invisible decay into a pair of dark matter plus mono-jet. We have illustrated that a sizable coupling of the radion to dark matter is necessary in the parameter space that can accommodate the diphoton excesses by photon-jets.

Acknowledgments

We would like to thank Veronica Sanz for helpful discussions during the project. The work of CH is supported by the World Premier International Research Center Initiative (WPI Initiative), MEXT, Japan. The work of HML is supported in part by Basic Science Research Program through the National Research Foundation of Korea (NRF) funded by the Ministry of Education, Science and Technology(2013R1A1A2007919). MP is supported by IBS under the project code, IBS-R018-D1.

Appendix: Couplings between radion and KK graviton

In this appendix, we provide the details for the triple self-couplings between the radion and the KK graviton. The couplings between these two fields come from the gravity self-interactions in 5D. For the warped metric,

$$ds^2 = w^2(y)\mathcal{G}_{\mu\nu}dx^\mu dx^\nu + G_{55}dy^2 \equiv G_{MN}dx^M dx^N \tag{A.1}$$

with $\mathcal{G}_{\mu\nu} = e^{-2\hat{r}}\hat{g}_{\mu\nu}$ and $G_{55} = -(1+2\hat{r})^2$, the 4D components of the Einstein tensor are

$$R_{\mu\nu}(\mathcal{G}) = R_{\mu\nu}(\hat{g}) + 2(\partial_\mu\hat{r}\partial_\nu\hat{r} + \partial_\mu\partial_\nu\hat{r}) + \eta_{\mu\nu}(\Box\hat{r} - 2(\partial\hat{r})^2). \tag{A.2}$$

In linearized gravity with $\hat{g}_{\mu\nu} = \eta_{\mu\nu} + \hat{G}_{\mu\nu}$, we get

$$\begin{aligned} R_{\mu\nu}(\hat{g}) &= \partial_\mu\partial_\nu\hat{G}^{\mu\nu} - \Box\hat{G} + \frac{1}{2}\hat{G}^{\mu\nu}\Big(\Box\hat{G}_{\mu\nu} + \partial_\mu\partial_\nu\hat{G} - \partial_\lambda\partial_\mu\hat{G}^\lambda_\nu - \partial_\lambda\partial_\nu\hat{G}^\lambda_\mu\Big) + \cdots, & \text{(A.3)} \\ \sqrt{-\hat{g}} &= 1 + \frac{1}{2}\hat{G} - \frac{1}{4}\Big(\hat{G}^{\mu\nu}\hat{G}_{\mu\nu} - \frac{1}{2}\hat{G}^2\Big) + \cdots & \text{(A.4)} \end{aligned}$$

where $\hat{G} \equiv \eta^{\mu\nu}\hat{G}_{\mu\nu}$ and $\cdots$ are higher order terms for $\hat{G}_{\mu\nu}$. Then, the effective Lagrangian for the KK graviton and the radion is

$$\begin{aligned} \mathcal{L}_{\text{eff}} &= \int dy\, w^2(1+2\hat{r})e^{-4\hat{r}}\sqrt{-\hat{g}}\Big[e^{2\hat{r}}(\eta^{\mu\nu} - \hat{G}^{\mu\nu})R_{\mu\nu}(\mathcal{G}) + G^{55}R_{55}(G)\Big] & \text{(A.5)} \\ &= \int dy\, w^2\Big[-\frac{1}{2}\hat{G}\Box\hat{G} + \frac{1}{2}\hat{G}^{\mu\nu}(\Box G_{\mu\nu} + \partial_\mu\partial_\nu\hat{G} - \partial_\lambda\partial_\mu\hat{G}^\lambda_\nu - \partial_\lambda\partial_\nu\hat{G}^\lambda_\mu\Big) - 6(\partial\hat{r})^2 \\ &\quad -2\hat{G}^{\mu\nu}\partial_\mu\hat{r}\partial_\nu\hat{r} - 3\hat{G}(\partial\hat{r})^2 - 2\hat{r}^2(\partial_\mu\partial_\nu\hat{G}^{\mu\nu} - \Box\hat{G}) + \frac{3}{2}(\hat{G}^{\mu\nu}\hat{G}_{\mu\nu} - \frac{1}{2}\hat{G}^2)\Box\hat{r} + \cdots\Big]. \end{aligned}$$

Here, we note that the radion-KK graviton mixing terms are eliminated by the field definition of the graviton [36]. As a consequence, the triple couplings between KK graviton and radion are

$$\begin{aligned} \mathcal{L}_{rr} &= -2\int dy\, w^2\Big[\hat{G}^{\mu\nu}\partial_\mu\hat{r}\partial_\nu\hat{r} + \frac{3}{2}\hat{G}(\partial\hat{r})^2 + \hat{r}^2(\partial_\mu\partial_\nu\hat{G}^{\mu\nu} - \Box\hat{G})\Big], & \text{(A.6)} \\ \mathcal{L}_{GG} &= \frac{3}{2}\int dy\, w^2\Big(\hat{G}^{\mu\nu}\hat{G}_{\mu\nu} - \frac{1}{2}\hat{G}^2\Big)\Box\hat{r}. & \text{(A.7)} \end{aligned}$$

Then, by inserting the bulk profiles for the KK graviton and the radion from (15), the above triple effective interactions become

$$\mathcal{L}_{rr} = -\frac{c_{rr}}{\Lambda}\left[G^{\mu\nu}\partial_\mu r\partial_\nu r + \frac{3}{2}G(\partial r)^2 + r^2(\partial_\mu\partial_\nu G^{\mu\nu} - \Box G)\right], \tag{A.8}$$

$$\mathcal{L}_{GG} = \frac{c_{GG}}{\Lambda}\Big(G^{\mu\nu}G_{\mu\nu} - \frac{1}{2}G^2\Big)\Box r \tag{A.9}$$

where

$$c_{rr} = \int dy\, w^2 (f_r)^2 (f_G^{(n)}) = \frac{1}{3(x_n^G)^4 |J_2(x_n^G)|}\int_0^{x_n^G} dz\, z^3 J_2(z) \tag{A.10}$$

$$c_{GG} = \int dy\, w^2 (f_r)(f_G^{(n)})^2 = \frac{\sqrt{6}}{4(x_n^G)^4 (J_2(x_n^G))^2}\int_0^{x_n^G} dz\, z^3 (J_2(z))^2. \tag{A.11}$$

For generality, we also include the decay rate of the radion into a pair of KK gravitons, if kinematically allowed,

$$\Gamma_r(GG) = \frac{c_{GG}^2\, m_r^3}{32\pi\Lambda^2}\left(20 - \frac{40}{3}\frac{m_r^2}{m_G^2} + \frac{46}{9}\frac{m_r^4}{m_G^4} - \frac{8}{9}\frac{m_r^6}{m_G^6} + \frac{1}{9}\frac{m_r^8}{m_G^8}\right)\left(1 - \frac{4m_G^2}{m_r^2}\right)^{\frac{1}{2}}. \tag{A.12}$$

References

[1] ATLAS Collaboration, ATLAS-CONF-2015-081; CMS Collaboration, CMS PAS EXO-15-004; ATLAS collaboration, ATLAS-CONF-2016-018; CMS Collaboration, CMS-PAS-EXO-16-018.

[2] R. Franceschini *et al.*, arXiv:1512.04933 [hep-ph]; J. Ellis, S. A. R. Ellis, J. Quevillon, V. Sanz and T. You, arXiv:1512.05327 [hep-ph].

[3] D. M. Ghilencea and H. M. Lee, arXiv:1606.04131 [hep-ph].

[4] C. Han, H. M. Lee, M. Park and V. Sanz, Phys. Lett. B **755** (2016) 371 doi:10.1016/j.physletb.2016.02.040 [arXiv:1512.06376 [hep-ph]].

[5] M. T. Arun and P. Saha, arXiv:1512.06335 [hep-ph]; J. S. Kim, K. Rolbiecki and R. R. de Austri, arXiv:1512.06797 [hep-ph]; M. R. Buckley, arXiv:1601.04751 [hep-ph]; A. Martini, K. Mawatari and D. Sengupta, arXiv:1601.05729 [hep-ph]; C. Q. Geng and D. Huang, arXiv:1601.07385 [hep-ph]; V. Sanz, arXiv:1603.05574 [hep-ph]; A. Falkowski and J. F. Kamenik, arXiv:1603.06980 [hep-ph]; J. L. Hewett and T. G. Rizzo, arXiv:1603.08250 [hep-ph].

[6] S. Knapen, T. Melia, M. Papucci and K. Zurek, Phys. Rev. D **93** (2016) no.7, 075020 doi:10.1103/PhysRevD.93.075020 [arXiv:1512.04928 [hep-ph]].

[7] P. Agrawal, J. Fan, B. Heidenreich, M. Reece and M. Strassler, arXiv:1512.05775 [hep-ph]; J. Chang, K. Cheung and C. T. Lu, arXiv:1512.06671 [hep-ph]; F. Domingo, S. Heinemeyer, J. S. Kim and K. Rolbiecki, arXiv:1602.07691 [hep-ph]; M. Badziak, M. Olechowski, S. Pokorski and K. Sakurai, arXiv:1603.02203 [hep-ph]. Y. Jiang, L. Li and R. Zheng, arXiv:1605.01898 [hep-ph].

[8] B. Dasgupta, J. Kopp and P. Schwaller, Eur. Phys. J. C **76** (2016) 277 doi:10.1140/epjc/s10052-016-4127-4 [arXiv:1602.04692 [hep-ph]].

[9] S. M. Choi, Y. J. Kang and H. M. Lee, arXiv:1605.04804 [hep-ph].

[10] L. Randall and R. Sundrum, Phys. Rev. Lett. **83** (1999) 3370 doi:10.1103/PhysRevLett.83.3370 [hep-ph/9905221].

[11] C. Csaki, M. Graesser, L. Randall and J. Terning, Phys. Rev. D **62** (2000) 045015 doi:10.1103/PhysRevD.62.045015 [hep-ph/9911406]; C. Csaki, M. L. Graesser and G. D. Kribs, Phys. Rev. D **63** (2001) 065002 doi:10.1103/PhysRevD.63.065002 [hep-th/0008151].

[12] H. Davoudiasl, J. L. Hewett and T. G. Rizzo, Phys. Rev. D **63** (2001) 075004 doi:10.1103/PhysRevD.63.075004 [hep-ph/0006041]; T. G. Rizzo, JHEP **0206** (2002) 056 doi:10.1088/1126-6708/2002/06/056 [hep-ph/0205242].

[13] C. Csaki, J. Hubisz and S. J. Lee, Phys. Rev. D **76** (2007) 125015 doi:10.1103/PhysRevD.76.125015 [arXiv:0705.3844 [hep-ph]].

[14] H. M. Lee, M. Park and V. Sanz, Eur. Phys. J. C **74** (2014) 2715 [arXiv:1306.4107 [hep-ph]]; JHEP **1405** (2014) 063 [arXiv:1401.5301 [hep-ph]].

[15] P. Cox, A. D. Medina, T. S. Ray and A. Spray, arXiv:1512.05618 [hep-ph]; A. Ahmed, B. M. Dillon, B. Grzadkowski, J. F. Gunion and Y. Jiang, arXiv:1512.05771 [hep-ph].

[16] J. F. Donoghue, J. Gasser and H. Leutwyler, Nucl. Phys. B **343** (1990) 341. doi:10.1016/0550-3213(90)90474-R

[17] F. Bezrukov and D. Gorbunov, JHEP **1005** (2010) 010 doi:10.1007/JHEP05(2010)010 [arXiv:0912.0390 [hep-ph]].

[18] J. D. Clarke, R. Foot and R. R. Volkas, JHEP **1402** (2014) 123 doi:10.1007/JHEP02(2014)123 [arXiv:1310.8042 [hep-ph]].

[19] K. Mimasu and V. Sanz, JHEP **1506** (2015) 173 doi:10.1007/JHEP06(2015)173 [arXiv:1409.4792 [hep-ph]].

[20] J. Jaeckel and M. Spannowsky, Phys. Lett. B **753** (2016) 482 doi:10.1016/j.physletb.2015.12.037 [arXiv:1509.00476 [hep-ph]].

[21] B. M. Dillon, D. P. George and K. L. McDonald, arXiv:1605.03087 [hep-ph].

[22] T. A. collaboration, *Search for new phenomena in the dilepton final state using proton-proton collisions at ? s = 13 TeV with the ATLAS detector*, *ATLAS-CONF-2015-070* (2015).

[23] **ATLAS** Collaboration, G. Aad et al., *Search for an additional, heavy Higgs boson in the $H \to ZZ$ decay channel at $\sqrt{s} = 8$ TeV in pp collision data with the ATLAS detector*, *Eur. Phys. J.* **C76** (2016), no. 1 45.

[24] **CMS** Collaboration, V. Khachatryan et al., *Search for a Higgs Boson in the Mass Range from 145 to 1000 GeV Decaying to a Pair of W or Z Bosons*, *JHEP* **10** (2015) 144.

[25] **ATLAS** Collaboration, T. A. collaboration, *A search for resonant Higgs-pair production in the $b\bar{b}b\bar{b}$ final state in pp collisions at $\sqrt{s} = 8$ TeV*, .

[26] T. A. collaboration, *Search for heavy resonances decaying to a Z boson and a photon in pp collisions at $\sqrt{s} = 13$ TeV with the ATLAS detector*, *ATLAS-CONF-2016-010* (2016).

[27] **CMS** Collaboration, S. Chatrchyan et al., *Searches for new physics using the $t\bar{t}$ invariant mass distribution in pp collisions at $\sqrt{s}$=8 TeV*, *Phys. Rev. Lett.* **111** (2013), no. 21 211804. [Erratum: Phys. Rev. Lett.112,no.11,119903(2014)].

[28] B. M. Dillon and V. Sanz, arXiv:1603.09550 [hep-ph].

[29] S. Y. Choi, M. M. Muhlleitner and P. M. Zerwas, Phys. Lett. B **718**, 1031 (2013) doi:10.1016/j.physletb.2012.11.050 [arXiv:1209.5268 [hep-ph]]; P. Artoisenet *et al.*, JHEP **1311**, 043 (2013) doi:10.1007/JHEP11(2013)043 [arXiv:1306.6464 [hep-ph]].

[30] G. Panico, L. Vecchi and A. Wulzer, arXiv:1603.04248 [hep-ph]; M. Fabbrichesi, M. Pinamonti and A. Urbano, arXiv:1604.06948 [hep-ph].

[31] P. Cox, A. D. Medina, T. S. Ray and A. Spray, JHEP **1402** (2014) 032 doi:10.1007/JHEP02(2014)032 [arXiv:1311.3663 [hep-ph]].

[32] R. Contino, Y. Nomura and A. Pomarol, Nucl. Phys. B **671** (2003) 148 doi:10.1016/j.nuclphysb.2003.08.027 [hep-ph/0306259]; K. Agashe, R. Contino and A. Pomarol, Nucl. Phys. B **719** (2005) 165 doi:10.1016/j.nuclphysb.2005.04.035 [hep-ph/0412089]; R. Contino, doi:10.1142/97898143271830005 arXiv:1005.4269 [hep-ph]; R. Contino, L. Da Rold and A. Pomarol, Phys. Rev. D **75** (2007) 055014 doi:10.1103/PhysRevD.75.055014 [hep-ph/0612048]; P. R. Archer, arXiv:1403.8048 [hep-ph]. D. Croon, B. M. Dillon, S. J. Huber and V. Sanz, arXiv:1510.08482 [hep-ph].

[33] J. Alwall *et al.*, JHEP **1407**, 079 (2014) doi:10.1007/JHEP07(2014)079 [arXiv:1405.0301 [hep-ph]].

[34] https://atlas.web.cern.ch/Atlas/GROUPS/PHYSICS/PLOTS/EGAM-2015-004/

[35] S. D. Ellis, T. S. Roy and J. Scholtz, Phys. Rev. D **87** (2013) no.1, 014015 doi:10.1103/PhysRevD.87.014015 [arXiv:1210.3657 [hep-ph]].

[36] G. F. Giudice, R. Rattazzi and J. D. Wells, Nucl. Phys. B **544** (1999) 3 doi:10.1016/S0550-3213(99)00044-9 [hep-ph/9811291]